第 25 卷第 8 期 无 机 化 学 学 报 Vol.25 No.8
2009 年 8 月 CHINESE JOURNAL OF INORGANIC CHEMISTRY 1379~1383

锂离子电池正极材料 $LiV_{3-x}Al_xO_8$ 的水热合成与性能

冯季军*,[1,2] 刘晓贞[1] 刘祥哲[1] 张晓梅[2] 姜建壮[2] 赵 静[1,2] 王 敏[1]
([1]济南大学化学化工学院,济南 250022)
([2]山东大学化学与化工学院,济南 250100)

摘要:采用水热法制备了 Al 掺杂的锂二次电池正极材料 $LiV_{3-x}Al_xO_8$,并用 X 射线衍射和扫描电镜对材料的晶体结构和形貌进行了表征。以 50 mA·g^{-1} 进行恒流充放电测试,结果表明 Al 掺杂能够明显改善材料的电化学性能。在掺杂改性的 $LiV_{3-x}Al_xO_8$ 材料中,$LiV_{2.93}Al_{0.07}O_8$ 的初始容量最高,达到 325 mAh·g^{-1}。当掺杂量为 x=0.04 时,材料的循环性能最佳。$LiV_{2.96}Al_{0.04}O_8$ 经 20 次循环后仍保持 179 mAh·g^{-1} 的比容量,且充放电效率始终维持在 98%左右。

关键词:正极材料;水热合成;钒酸锂;掺杂
中图分类号:O614.111 **文献标识码**:A **文章编号**:1001-4861(2009)08-1379-05

Hydrothermal Synthesis of $LiV_{3-x}Al_xO_8$ and Its Performance as Positive Electrode Material for Lithium-Ion Batteries

FENG Ji-Jun*,[1,2] LIU Xiao-Zhen[1] LIU Xiang-Zhe[1] ZHANG Xiao-Mei[2]
JIANG Jian-Zhuang[1] ZHAO Jing[1,2] WANG Min[1]
([1]*School of Chemistry and Chemical Engineering, University of Jinan, Jinan* 250022)
([2]*School of Chemistry and Chemical Engineering, Shandong University, Jinan* 250100)

Abstract: Al doped lithiated vanadium oxides $LiV_{3-x}Al_xO_8$ as promising positive electrode material for secondary lithium batteries are prepared with a hydrothermal process. The crystalline phase is characterised by powder X-ray diffraction and the morphology is observed by scanning electron microscope. The electrochemical properties of synthesized samples are investigated by galvanostatic charge and discharge at a current density of 50 mA·g^{-1}. The electrochemical properties were greatly improved via Al doping. Among the doping modified material $LiV_{3-x}Al_xO_8$, the maximal initial specific discharge capacity belongs to $LiV_{2.93}Al_{0.07}O_8$ which can attain 325 mAh·g^{-1}. The most excellent performance can be achieved when x=0.04. The $LiV_{2.96}Al_{0.04}O_8$ material preserves a high charge-discharge efficiency of around 98% and keep a special capacity of 179 mAh·g^{-1} after 20 cycles.

Key words: positive electrode material; hydrothermal synthesis; lithium trivanadate; doping

The layered $LiCoO_2$ has been the dominating positive electrode material for commercial lithium ion cells in the decade or so since its facility to manufacture and good cycling behaviour. But only 50% of its theoretical capacity could be utilized in practical cells due to chemical and structural instabilities at deep charge with $(1-x)<0.5$ in $Li_{1-x}CoO_2$[1,2]. Charged $Li_{1-x}CoO_2$ poses safety concerns due to the highly oxidized nature of the Co^{3+}/Co^{4+} couple and an overlap of the Co^{3+}/Co^{4+}: 3*d* band with the top of the O^{2-}: 2*p* band. Moreover, Co

收稿日期:2009-03-30。收修改稿日期:2009-06-23。
国家自然科学基金(No.20573047),山东省自然科学基金(No.Y2008B64)和山东省优秀中青年科学家奖励基金(No.2006BS09001)资助项目。
*通讯联系人。E-mail:chm_fengjj@ujn.edu.cn
第一作者:冯季军,女,32 岁,博士,讲师;研究方向:能源材料。

is expensive and relatively toxic. These difficulties have generated enormous interests in the development of alternative positive electrode materials. In this regard, cation-substituted spinel manganese oxides $LiMn_2O_4$[3~5], conductive carbon incorporated olivine iron phosphate $LiFePO_4$[6~8] and layered oxide solid solutions $LiMn_xNi_xCo_{1-2x}O_2$[9~11] are being intensively pursued continuously. These are safer and potentially cheaper than $LiCoO_2$. However, it is a perception that there is little scope for further increases in capacity with the existing positive electrode materials.

Vanadium oxides are attractive alternatives as vanadium is known to exist in a wide range of oxidation states from +2 as in VO to +5 as in V_2O_5 and the vanadium oxides have the potential to offer much higher capacities. Among the various known vanadium oxides, LiV_3O_8 have been found to show interesting properties both as positive electrode materials and as negative electrode materials in aqueous rechargeable lithium battery[12]. LiV_3O_8 has a layered structure where pre-existing Li^+ ions at octahedral sites attaching adjacent layers strongly. Over three equivalents of Li^+ ions can be inserted/extracted in LiV_3O_8 reversibly because of both the outstanding structural stability and empty sites for Li^+ ion occupation between the layers. Moreover, the LiV_3O_8 shows superior safety characteristics compared to the $LiCoO_2$ as the V^{3+}/V^{4+} 3*d* or V^{4+}/V^{5+} 3*d* band lie well above the O^{2-} 2*p* band.

Critical to the success of new positive electrode materials, is their preparation, which controls the morphology, particle size and cation order amongst other critical parameters[13]. Although traditionally high temperature methods have been widely used for their simpleness, they are energy intensive and cannot readily produce many potentially metastable structures that might result in high lithium ion diffusivity. Soft chemical approaches, such as hydrothermal/solvothermal or ion-exchange offer many advantages.

One of the effective methods to improve the cycle performance of positive electrode materials is doping with heteroatoms[14,15]. In this work, a serials of Al doped LiV_3O_8 have been synthesized via a hydrothermal process. The crystal structure of $LiV_{3-x}Al_xO_8$ (x=0, 0.01, 0.02, 0.04, 0.07, 0.10) were refined by powder X-ray diffraction and the micromorphology was characterized using scanning electron microscopy. By performing the galvanostatic charge and discharge experiments, their electrochemical properties were systematically investigated and compared.

1 Experimental

1.1 Materials preparation

Analytically pure $LiOH \cdot H_2O$, V_2O_5, $AlCl_3$ and $NH_3 \cdot H_2O$ were used as raw materials without any purification. Stoichiometrical $LiOH \cdot H_2O$, V_2O_5 and $AlCl_3$ were weighed and mixed in deionized water followed by ammonia (1∶10) adding slowly to adjust the pH value to 9 with magnetic stirring and heating in water bath. The obtained dark green solution was then transferred into a 50 mL teflon lined autoclave. The autoclave was sealed, and heated at 160 ℃ for 16 h. After hydrothermal treatment, a colorless clear solution was obtained in which pH decreased to 7. The solution was dried in air at 100 ℃ to evaporate the water. The precursor was then heat-treated at 300 ℃ for 12 h. After natural cooling in the furnace, the dark brown products were finally gained.

1.2 Characterization of samples

The X-ray diffraction (XRD) analysis was operated on Bruker AXS D8 Advance X-ray diffractometer with Cu $K\alpha$ radiation in the 2θ range of 10°~80° to identify the crystalline phase of synthesized $LiV_{3-x}Al_xO_8$ powders. Morphology of the samples was observed with the Hitachi S-2500 Scanning Electron Microscope.

The $LiV_{3-x}Al_xO_8$ materials were mixed with acetylene black and polytetrafluoroethylene (PTFE) in a weight ratio of 80∶12∶8. The aforementioned mixture was ultrasonic dispersed in ethanol. The as-prepared slurry was coated onto an aluminum foil and pressed at 10 MPa, and then vacuum dried at 120 ℃ for 12 h to obtain the positive electrodes. Electrochemical experiments were operated on CR2032 coin cells with thus fabricated positive electrodes, lithium metal pellets as anode electrodes, 1 $mol \cdot L^{-1}$ $LiPF_6$ in EC+DMC (1∶1 volume ratio) as electrolytes and Celgard 2300 membrane as separators. All cells were assembled in an argon-filled

glove box (Mikrouna Super 1220/750/900). The galvanostatically charge-discharge tests were performed on PCBT-138-32D battery program-control test system with a mass current density of 50 $mA \cdot g^{-1}$ between the potential limits of 1.5~4.0 V (vs Li/Li^+).

2 Results and discussion

2.1 Crystal structure

The XRD patterns of $LiV_{3-x}Al_xO_8$ (x=0, 0.02, 0.07, 0.10) are shown in Fig.1 and the refined data of these samples are listed in Table 1. The XRD patterns indicate that all samples are identified as single-phase layered structures corresponding to the LiV_3O_8 (PDF#72-1193). The LiV_3O_8 has monoclinic crystalline and belongs to the $P2_1/m$ space group. It is composed of two basic structural units, namely, a VO_6 octahedron and a VO_5 distorted trigonal bipyramids. According to the XRD patterns, the decreased diffraction intensity and widen peaks with lager values of full width at half peak (FWHP) indicate the crystallinity decline with the increasing doping concentration. The XRD patterns exhibit that all the $LiV_{3-x}Al_xO_8$ samples have shifts of the 2θ of the (100) peak to larger values in contrast with the pristine LiV_3O_8. It is also noteworthy that the Al doped materials have much smaller $d_{(100)}$ values than the undoped LiV_3O_8. The small $d_{(100)}$ value lead to relatively short diffusion paths for the lithium ions inserted between these planes. Therefore, the improved electrochemical performance should be expected for the $LiV_{3-x}Al_xO_8$ materials.

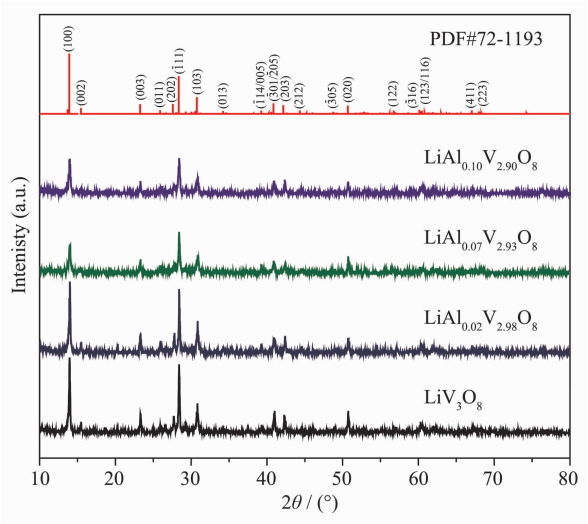

Fig.1　XRD patterns of $LiV_{3-x}Al_xO_8$ powders

Table 1　Refined data of $LiV_{3-x}Al_xO_8$ samples

x in $LiV_{3-x}Al_xO_8$	2θ / (°)	$d_{(100)}$ / nm	FWHP / (°)
0	13.924	0.635 50	0.170
0.02	14.001	0.632 01	0.180
0.07	14.000	0.632 04	0.273
0.10	13.980	0.632 96	0.228
PDF	13.915	0.635 91	—

2.2 Morphology

Fig.2 shows the morphology of hydrothermal synthesized LiV_3O_8 in different magnification from 1 000× to 7 000×. It can be seen that the sample consists of agglomerations of widely dispersed small particles. In Fig.2(C) we can clearly see submicron-sized plate-like

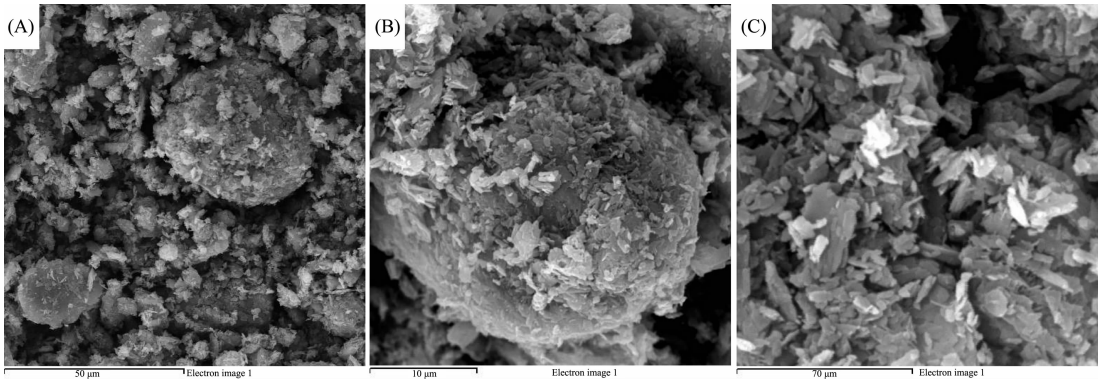

(A) in 1 000×; (B) in 3 000×; (C) in 7 000×

Fig.2　SEM images of hydrothermal synthesized LiV_3O_8 in different magnification

particles with agglomeration. It has been reported that the intercalation process of Li^+ ion between the layers of positive electrode material is a diffusion process[16~18]. Therefore the larger grains would lead to a long path for Li^+ ion, which are disadvantageous to intercalation. By contrast, the floppy morphology with smaller grains is beneficial to lithium-ion intercalation and deintercalation, leading to better electrochemical performance.

2.3 Test of electrochemical performance

The first discharge curves and corresponding differential curves of $LiV_{3-x}Al_xO_8$ (x=0, 0.01, 0.02, 0.04, 0.07, 0.10) were illustrated in Fig.3. In the discharge curves, both the intercalation of Li^+ ion (the left axis) and the special capacity (the right axis) were shown simultaneously as functions of battery voltage. The calculated differential capacities dQ/dV were also demonstrated as functions of battery voltage. It can be seen in Fig.3 that the Al doped lithium trivanadate materials take on larger initial capacities than the pristine LiV_3O_8 except for the $LiV_{2.90}Al_{0.10}O_8$. Among the doped materials, the $LiV_{2.93}Al_{0.07}O_8$ presents the maximal initial specific capacity of 325 mAh·g^{-1} correlated to about 3.5 additional Li^+ inserted per formula unit. By contrast, the $LiV_{2.90}Al_{0.10}O_8$ shows an initial specific capacity of 275 mAh·g^{-1}, which is a little less than the LiV_3O_8′s 282 mAh·g^{-1}.

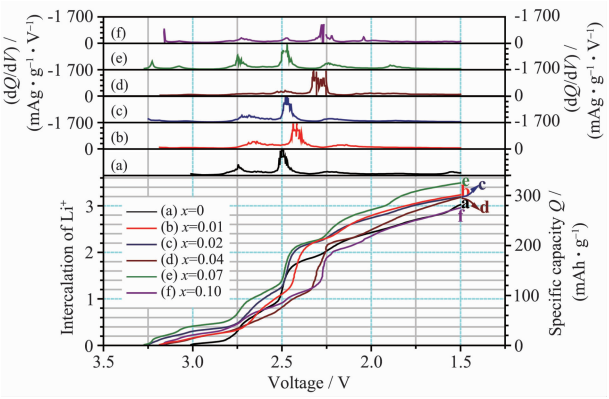

Fig.3 Initial discharge curves of $LiV_{3-x}Al_xO_8$

The features of the initial discharge process can be more finely represented in the derivative curves in Fig. 3. From the open circuit voltage to about 2.8 V, the lithium intercalation proceeds as a single-phase reaction, exhibited rather clearly by the smooth platform in corresponding differential curves. During this period, $LiV_{3-x}Al_xO_8$ shows section capacities of 30~50 mAh·g^{-1} while the LiV_3O_8 shows a distinctly lower section capacity of only 14 mAh·g^{-1}. Only 0.15 Li^+ was allowed to insert into this undoped material until the battery voltage descend to 2.8 V. In the voltage region of 2.8~2.5 V, the battery voltage shows nearly independence on the composition which exhibited as a peak in the corresponding differential curve. This indicates two-phase reactions occurred in this region. In the differential curves of $LiV_{2.93}Al_{0.07}O_8$, two distinct peaks respectively located in 2.7 V and 2.5 V can be detected. This phenomenon denotes the two-period discharge process of these materials. It is noticeable that $LiV_{2.93}Al_{0.07}O_8$ has an extraordinarily higher part special capacity of 50 mAh·g^{-1} at the voltage plateau of about 2.7 V, assuming 0.53 Li^+ intercalation. As to $LiV_{2.96}Al_{0.04}O_8$ and $LiV_{2.90}Al_{0.10}O_8$, the two-phase reactions shift to a lower voltage of about 2.3 V.

The cycle performance of $LiV_{3-x}Al_xO_8$ (x=0, 0.01, 0.02, 0.04, 0.07, 0.10) were shown in Fig.4. The special capacity was shown in Fig.4, and the charge-discharge efficiency was demonstrated in the inset. It can be easily seen from Fig.4 that remarkably improved cycle performance can be achieved via Al doping. The undoped LiV_3O_8 shows a rapid capacity fading after 13 cycles, while the $LiV_{2.99}Al_{0.01}O_8$′s discharge capacity sharply declined after 16 cycles. Corresponding to that, these two materials present an unexpected fall of charge-discharge efficiency. This may due to the breakdown of the intercalation-extraction channels. When the doping amount x is more than 0.02, the $LiV_{3-x}Al_xO_8$ can cycle stably. Among them, $LiV_{2.96}Al_{0.04}O_8$ has the most

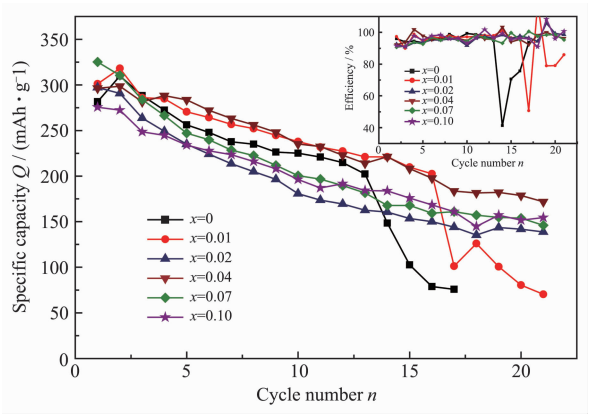

Fig.4 Cycle performance of $LiV_{3-x}Al_xO_8$

excellent cycle ability, which can preserve a special capacity of 179 mAh·g^{-1} after 20 cycles. When x=0.02, 0.07 and 0.10, the special capacities remain 142, 154 and 152 mAh·g^{-1} respectively after 20 cycles. Furthermore, the $LiV_{3-x}Al_xO_8$ materials, with x in the range of 0.02 to 0.10, all kept good charge-discharge efficiency above 90% and sometimes even near 100%.

3 Conclusions

A hydroth ermal method was employed to synthesize $LiV_{3-x}Al_xO_8$ with x in the range of $0 \leqslant x \leqslant 0.10$. All samples are identified as single-phase layered structures consistent with the LiV_3O_8. Al doped lithiated vanadium oxides show obviously improved cycle reversibility compared to the pristine LiV_3O_8. Among the doped materials, $LiV_{2.93}Al_{0.07}O_8$ shows a maximal initial specific capacity of 325 mAh·g^{-1} and $LiV_{2.96}Al_{0.04}O_8$ take on the most excellent cycle ability keeping a special capacity of 179 mAh·g^{-1} after 20cycles. The doped materials also show excellent reversibility with high charge-discharge efficiency during cycling. The Al doping modified lithium trivanadate materials are promising for application in lithium ion batteries.

References:

[1] Jarvis C R, Lain M J, Gao Y, et al. *J. Power Sources*, **2005**, **146**:331~334

[2] Kannan A M, Manthiram A. *J. Power Sources*, **2006**,**159**:1405~1408

[3] Zhang L, Yabu T, Taniguchi I. *Mater. Res. Bull.*, **2009**,**44**:707~713

[4] FENG Ji-Jun(冯季军), XU Rong-Qi(徐荣琪), TANG Zhi-Yuan(唐致远), et al. *Chem. J. Chinese Universities* (*Gaodeng Xuexiao Huaxue Xuebao*), **2007**,**28**(8):1532~1536

[5] Gnanaraj J S, Pol V G, Gedanken A, et al. *Electrochem. Commun.*, **2003**,**5**:940~945

[6] Maccario M, Croguennec L, Le C F, et al. *J. Power Sources*, **2008**,**183**:411~417

[7] Jayaprakash N, Kalaiselvi N. *Electrochem. Commun.*, **2007**,**9**:620~628

[8] YU Feng(于　锋), ZHANG Jing-Jie(张敬杰), YANG Yan-Feng(杨岩峰), et al. *Chinese J. Inorg. Chem.*(*Wuji Huaxue Xuebao*), **2009**,**25**(1):42~46

[9] Ohzuku T, Makimura Y. *Chem. Lett.*, **2001**,**30**:642~643

[10]Kobayashi H, Arachi Y, Emura S, et al. *J. Power Sources*, **2005**,**146**:640~644

[11]WANG Hai-Yan(王海燕), TANG Ai-Dong(唐爱东), HUANG Ke-Long(黄可龙), et al. *Chinese J. Inorg. Chem.*(*Wuji Huaxue Xuebao*), **2008**,**24**(4):593~599

[12]Wan G, Fu L, Zhao N, et al. *Angew. Chem. Int. Ed.*, **2007**,**46**:295~297

[13]Chen J, Wang S, Whittingham M S. *J. Power Sources*, **2007**, **174**:442~448

[14]Wu Y P, Rahm E, Holze R. *Electrochim. Acta*, **2002**,**47**:3491~3507

[15]TANG Zhi-Yuan(唐致远), FENG ji-Jun(冯季军), XU Guo-Xiang(徐国祥). *Acta Chim. Sinica*(*Huaxue Xuebao*), **2003**, **61**(8):1316~1318

[16]Nassau K, Murphy D W. *J. of Non-Crystalline Solids*, **1981**, **44**:297~304

[17]Liu L, Jiao L F, Sun J L, et al. *Electrochim. Acta*, **2008**,**53**:7321~7325

[18]Feng C Q, Huang L F, Guo Z P, et al. *J. Power Sources*, **2007**, **174**:548~551